



## DSPACE1103 Controller for PWM Control of Power Electronic Converters

---

R Amalrajan, R Gunabalan and Nilanjan Tewari

EasyChair preprints are intended for rapid dissemination of research results and are integrated with the rest of EasyChair.

November 7, 2019

# DSPACE1103 CONTROLLER FOR PWM CONTROL OF POWER ELECTRONIC CONVERTERS

Amalrajan R<sup>1</sup>, Gunabalan R<sup>1</sup> and Nilanjan Tewari<sup>1</sup>

<sup>1</sup>School of Electrical Engineering

Vellore Institute of Technology- Chennai

Chennai -600 127, TamilNadu, India.

amalrajan.r@2017vitstudent.ac.in

gunabalan.r@vit.ac.in

nilanjan.tewari@vit.ac.in

**Abstract.** This paper presents the overview and working procedure of dSPACE1103 controller and its applications for power electronics converters. The configuration and control desk parameter settings have been discussed in detail. The pulse width modulation (PWM) for duty cycle control of DC-DC converter and sinusoidal pulse width modulation (SPWM) for voltage and frequency control of DC-AC converter using real time interface (RTI) library blocks in dSPACE and MATLAB simulink blocks in MATLAB simulink environment are presented. The simple blocksets in simulink and RTI library are used to obtain the control signals in order to turn on and turn off the power semiconductor switches in converters. The programming skills and knowledge are not required to generate the control signals. The real time prototype implementation of DC-DC converter and DC-AC converter in MATLAB with dSPACE controller is presented. Experimental results are provided to enhance the performance of dSPACE controller.

**Keywords:** dSPACE1103 controller, DC-DC converter, DC-AC converter, Pulse Width Modulation (PWM), Sinusoidal Pulse width Modulation (SPWM).

## 1 Introduction

In the present scenario, the applications of DC-DC converter are increased in medical equipment [1], dc distribution [2]-[4] and standalone renewable energy systems [5]. Similarly DC-AC converter usage along with DC-DC converter is increased in hybrid electric vehicle [6]-[8], smart grid [9]-[11], solid state transformers [12]-[13] and inverter-based distributed generation system [14]-[16]. As photovoltaics, batteries and other renewable/alternative power sources continue their rapid growth, many inverter/converter topologies have been introduced in literatures [17]. The presence of

more number of semiconductor switches reduces the efficiency and reliability of power electronic converter/inverter [18]. A unified PWM concept was introduced in SPWM, space vector PWM (SVPWM) [19], discontinuous space vector PWM (DSVPWM) and applied to a 3-phase dual-buck inverter to reduce the computational burden when implemented by a digital signal processor (DSP) [20]. A new simple and easy to use low cost, flexible, high accuracy digital photovoltaic array simulator with buck converter was designed [21]. The non-linearity of I-V curve causes a higher order polynomial equation that increases the computational time, size of memory and cost of the DSP. A buck-boost DC-DC converter with PV emulator using multiple simple I-V polynomial equations was implemented in low cost 8-bit microcontroller to overcome computational difficulties [22].

To implement P, PI, PID and optimization techniques, control boards including field programmable gate array (FPGA), microcontroller and LabVIEW controller have been used. But these controllers could not be interfaced with MATLAB simulink during implementation. The regenerative braking and friction brake controller were integrated into the advanced vehicle simulator (ADVISOR) of electric vehicle (EV) and its performance was validated in real-time by LabVIEW real-time controller and hardware in the loop (HIL) test bench [23]. For efficiency improvement, these models can be implemented in dSPACE controller. DSPACE is widely used for planning, designing, execution of hardware and software and to improve the accuracy of the output. DSPACE is preferred mainly in mechatronic systems such as converter, inverter, multilevel inverter, and voltage and frequency (VFD) control for drive systems. This helps for development and testing activities in real time. The dSPACE controller is broadly applied in industries for controlling electric powered automobile and power electronics converters [24]. It is highly useful for engineers as it gives high accuracy while working with real time controllers, low power use, brief development period, and user-friendliness. The fuel cell (FC) model was implemented in MATLAB simulink and converted into a C program which was programmed into a dSPACE or eZdsp R2818 DSP controller [25]. The dSPACE controller was used for prototype design & testing and DSP controller was used for field testing. A new lightning search algorithm was loaded in dSPACE DS1104 controller board for low power applications [26]. A solar emulator with better dynamics was built for different irradiances using DS1104 controller [27]. The robustness of the controller was demonstrated with 20% load disturbance and 10% input disturbance in a solid state transformer using dSPACE 1104 controller and Opal-RT simulator [28]. The dSPACE1104 controller is a lowest version and researchers are using the higher version of dSPACE1103 controller. The HIL setup was projected to test the adaptive headlight concept using dSPACE1103 in xPC target box platform [29]. The vehicle state information was sent by digital to analog channels of DS1103 and received by analog to digital channels of xPC target box. The dSPACE1103 controller was used for DC motor speed control applications [30].

In above literatures [24]-[30], dSPACE was used to generate PWM/SPWM in power electronics converters. The configuration parameter settings and design procedure are required for better understanding. In this paper, a different approach to generate control signals for power electronic converters in MATLAB simulink with dSPACE1103 controller is presented with configuration settings of MATLAB and control desk. The

simulink block output is interfaced with real time DC-DC converter and three phase inverter using dSPACE1103 controller. The experimental setup and results of the converters are presented

## 2 Methodology

MATLAB and control desk have basic set of guidelines and few preliminary procedures. The major RTI library tools such as MASTER PPC and SLAVE DSP F240 are used to generate the control signal and interface the feedback signals. The RTI blocksets are used for pulse generation for DC-DC converter and DC-AC converter with simple simulink blocks. The model is built to obtain the control signal through dSPACE1103 controller output pins without delay in real time.

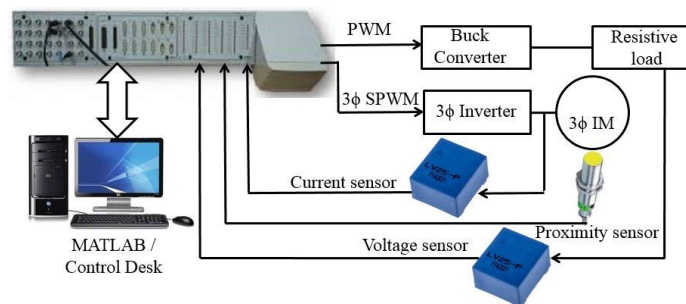


Fig 1. Block diagram

The simple block diagram of interfacing dSPACE controller with sensors and converters is shown in Fig. 1. The control desk is a software tool which is interfaced with MATLAB and RTI library. The RTI library is a software tool which is added to MATLAB library in order to generate control signal and to build MATLAB simulink model to get the simulation results through dSPACE1103 controller. Similarly, the signals from the sensors are feedback through dSPACE1103 to the MATLAB simulink blocks. Both control signal and feedback signal can be controlled and monitored in control desk. The dSPACE controller is used to transfer & interface control signal and feedback signal to both hardware and software. The dSPACE controller is connected with desktop and experimental setup which is controlled through control desk / MATLAB Simulink. The accessories of dSPACE1103 as shown in Fig. 2 consist of a connector and LED panels, controller board and license key. The connector and LED panels have easy access to I/O signals, ADC inputs, DAC outputs, Digital I/O, Slave DSP I/O, incremental encoder interfaces and serial interfaces. The RTI library in Fig. 3 has master PPC and slave DSP. The slave DSP simulink in-built blocks are used to generate pulses. The slave DSP, master PPC and MATLAB library simulink in-built blocks are used to develop a model for single phase pulse generation, three phase pulse generation and SPWM. The blocksets which are available in SLAVE DSP F240 and the corresponding output pin connection details are shown in Fig 4. The

master PPC simulink in-built blocks which are used to sense feedback signals and the corresponding output pin details in the digital I/O connector are indicated in Fig. 5.

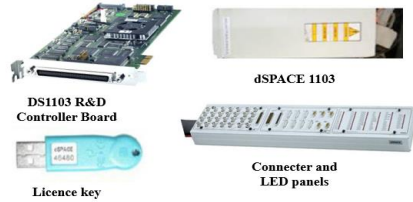


Fig 2. DSPACE1103 accessories

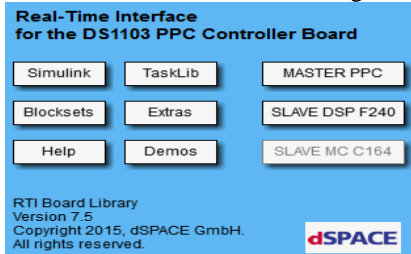
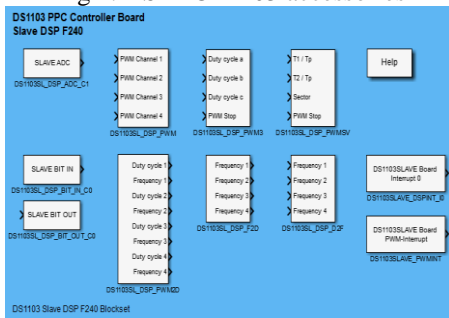
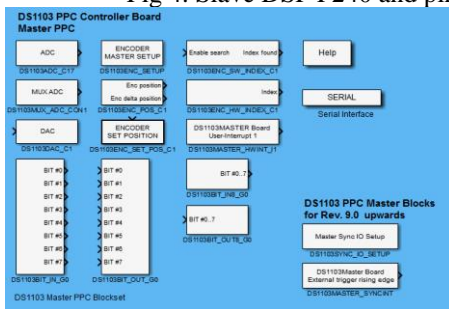


Fig 3. Real time interface (RTI) library



Slave I/O Connector (CP31)	Pin	Signal	Pin	Signal
	1	GND	20	GND
	2	SCAP1	21	SCAP2
	3	SCAP3	22	SCAP4
	4	GND	23	ST1PWM
	5	ST2PWM	24	ST3PWM
	6	GND	25	GND
	7	SPWM1	26	SPWM2
	8	SPWM3	27	SPWM4
	9	SPWM5	28	SPWM6
	10	SPWM7	29	SPWM8
	11	SPWM9	30	GND
	12	STMCLK	31	STMTRDIR
	13	GND	32	SPDPINT
	14	STINT1	33	STINT2
	15	GND	34	SSOMI
	16	SSIMO	35	SSTE
	17	SCLK	36	SBI0
	18	SXF	37	GND
	19	VCC (+5 V)		

Fig 4. Slave DSP F240 and pin details of slave I/O connector



Digital I/O Connector (CP30)	Pin	Signal	Pin	Signal	Pin	Signal
	17	GND	33	IO31	50	VCC (+5 V)
	16	IO30	32	IO29	49	RT3
	15	IO28	31	IO27	48	RT2
	14	IO26	30	IO25	47	RT1
	13	IO24	29	IO23	46	RT0
	12	IO22	28	IO21	45	GND
	11	IO20	27	IO19	44	GND
	10	IO18	26	IO17	43	GND
	9	IO16	25	IO15	42	GND
	8	IO14	24	IO13	41	GND
	7	IO12	23	IO11	40	GND
	6	IO10	22	IO9	39	GND
	5	IO8	21	IO7	38	GND
	4	IO6	20	IO5	37	GND
	3	IO4	19	IO3	36	GND
	2	IO2	18	IO1	35	GND
	1	IO0			34	GND

Fig 5. Master PPC and pin details of digital I/O connector

### 3 Design Steps In Matlab And Control Desk

In MATLAB simulink model, the following steps to be followed for configuring parameters and interfacing the control desk:

#### 3.1 MATLAB

1. Launch MATLAB version 2015a
2. Create a new simulink model
3. Design and save the model
4. Set the stop time(inf)
5. Open and edit the configuration parameters

6. Set the solver parameters
  - a. Solver\_ode1(euler)
  - b. Fixed step size multiples of sample time
  - c. Uncheck optimization
7. Set the hardware configuration to be.
  - a. Device vendor (Generic)
  - b. Device type(Custom)
  - c. integer (int)
  - d. floating point (float)
  - e. Byte ordering (BigEndien)
  - f. Signed integer division rounds to (zero)
8. Click apply & ok.
9. Build the model and verify the steps in diagnostics viewer. The build process should be 100% successful.
10. An .sdf file will be generated upon the completion of build process. On successful generation of .sdf file, the results will be validated in dSPACE ctrl\_desk.

### 3.2 dSPACE Control desk

1. Check the pulse results in the slave I/O connector
2. MATLAB simulation block can be found in “all variable descriptions”
3. Select .sdf file and choose model root
4. Drag and drop MATLAB blocks to dSPACE home screen
5. Choose appropriate measurement indicators.
6. Launch control desk on desktop
7. Create a new project and experiment
8. Choose names for project, root directory and experiment.
9. Add platform device DS1103 from the list
10. Import .sdf file (it will be available in MATLAB file save location)
11. After completion of above steps go online

## 4 PWM Generation

The PWM signal for DC-DC converter is generated using simple simulink blocks of RTI library. Fig. 6 indicates the single phase PWM generation using DS1103SL\_DSP\_PWM block in RTI library. DS1103SL\_DSP\_PWM, DS1103SL\_DSP\_PWM1, DS1103SL\_DSP\_PWM2 and DS1103SL\_DSP\_PWM3 blocks are used to generate constant duty cycle pulses for semiconductor switches 1 and 2. In DS1103SL\_DSP\_PWM and DS1103SL\_DSP\_PWM1 blocks, dead band period is not possible. In DS1103SL\_DSP\_PWM2 and DS1103SL\_DSP\_PWM3 blocks, user can set dead band limit up to 0-100 $\mu$ s.

The following steps are followed for PWM pulse generation:

- |        |   |                          |
|--------|---|--------------------------|
| Step 1 | : | go to new simulink model |
| Step 2 | : | go to RTI library        |

Step 3 : select the user requirement PWM simulink blocks

Step 4 : set the initialization limits

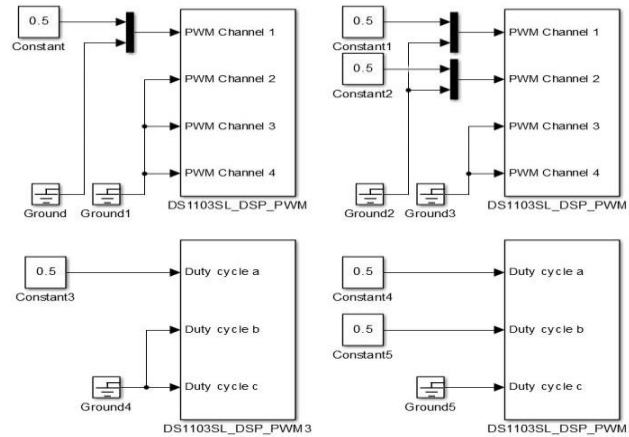


Fig 6. PWM generation for DC-DC Converter

The PWM block (DS1103SL\_DSP\_PWM and DS1103SL\_DSP\_PWM1) has four PWM channels and the output is obtained from slave I/O connector pins. A constant block is connected to the input signal which is used to generate constant duty cycle pulses. The reference signal is defined by the user. The user can set the switching frequency and can develop PWM simulink model. The magnitude of the carrier signal and reference signal limit is 0 to 1. The user can set the switching frequency from 1.25 Hz to 5 MHz, and set the duty cycle limit between 0 and 1. In Fig. 6, 0.5 in constant block indicates 50% duty cycle. Pulse output is obtained at slave I/O connector pins 5, 10, 29 and 11. The same procedure is followed for other PWM block (DS1103SL\_DSP\_PWM3 and DS1103SL\_DSP\_PWM2). It has three duty cycle connection ports with an additional feature for user to set dead band values for controlling the pulse signals. These PWM pulses are available in slave I/O pins 7 to 9 and inverted pulses are available in I/O pins 26 to 28. The pulse output voltage range is 4 V to 5 V.

## 5 Experimental Setup of DC-DC Converter

The buck converter is a step down DC-DC converter which is used for stepping down the input voltage in industry applications. Fig. 7 shows the experimental setup of a buck converter and real-time interfacing with dSPACE1103 controller. The buck converter operation depends on the switch position and inductor current. The dSPACE1103 controller is used to generate the switching pulses with a frequency of 20 kHz. Its input DC voltage is 20 V and a resistance of 25  $\Omega$  is connected across the load terminals. The specifications of the converter are given in Table 1.

Fig. 8 shows the switching frequency signal of buck converter and is observed in MDO\_3143 [Mixed Digital Oscilloscope]. The switching pulse waveform is taken for a duty cycle of 50% using DS1103SL\_DSP\_PWM3 block with a switching frequency

of 20 kHz. The amplitude of the pulse signal is increased to 14.8 V by a TLP 250 driver circuit.

Fig. 9 shows the closed loop simulation of a buck converter in MATLAB/simulink with PI controller. The simulink file is modified with real time interface RTI library of dSPACE1103 controller. The buck converter output voltage and duty cycles are measured. In dSPACE, the feedback voltage signal must be within  $\pm 10V$ . The output voltage is detected by using a potential divider and it is feedback through dSPACE1103 chip, via analog to digital converter [S1103MUX\_ADC\_CON1]. For the input voltage  $\pm 10V$ , the output value of ADC is  $\pm 1V$ ; MUX ADC is used to feed four different analog values. The output analog voltage of buck converter is converted into digital signal, which is verified in control desk. The digital pulse signal is connected via DAC. For the input range of  $\pm 1V$ , the output value of the DAC is  $\pm 10V$ .

Fig. 10 indicates the experimental results of buck converter viewed in dSPACE\_1103 control desk and the results captured in Tektronix MDO3024 for the output voltage of 8 V. During the run time, set voltage is varied and different output average voltages (actual Voltage) are captured in control desk. The results captured in Tektronix MDO3024 are shown in Fig. 11. a and Fig. 11. b. The reference voltage is set in the control desk directly. The set voltage and actual voltage calculations are verified in Fig. 10. b. and Fig. 11. b. using the well known formula  $V_o = \alpha * V_{dc}$ , where ' $\alpha$ ' is the duty cycle.

**Table 1 List of components**

Name of the Component	Specifications
IGBT [FGA25N120ANTD]	25A, 1200V
Diode [MUR 860]	8A, 600V
Inductor	184 $\mu H$ , 10A
Capacitor	220 $\mu F$ , 250V
Resistive load	25 $\Omega$

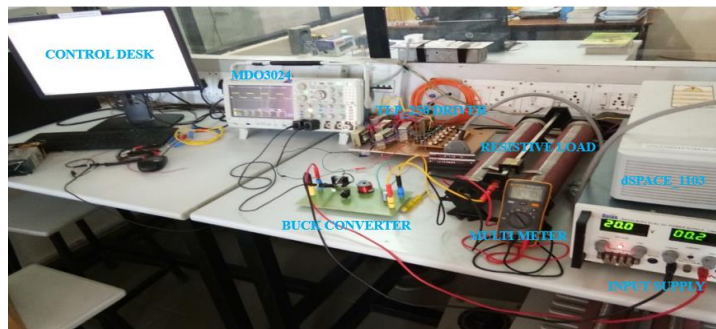


Fig. 7. Experimental setup for DC-DC converter



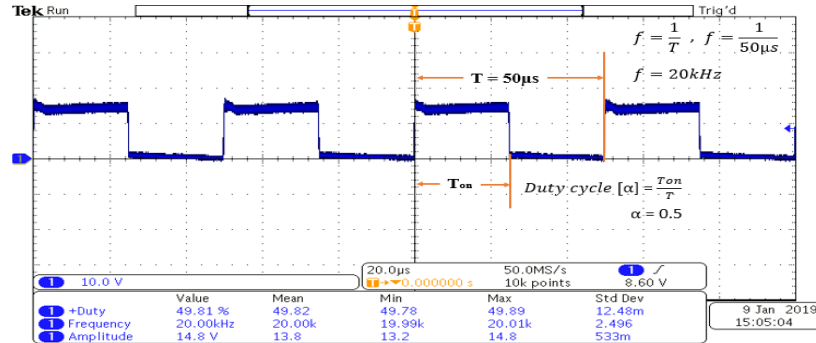


Fig 8. PWM waveform for  $\alpha = 0.5$  at 20 kHz switching frequency

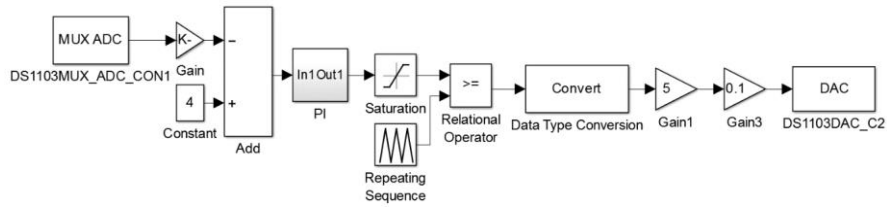


Fig 9. Closed loop simulation of DC-DC converter

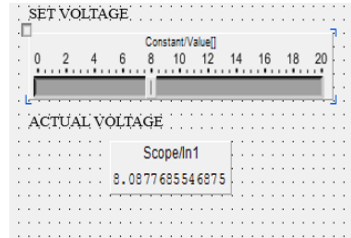


Fig 10. a. Set voltage and actual voltage in control desk

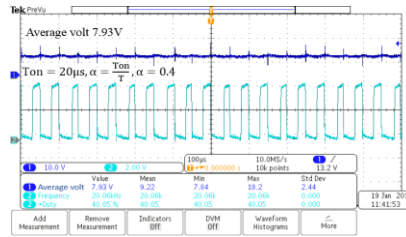


Fig 10. b. Duty cycle and output average voltage

Fig 10 Experimental results for  $V_o = 8\text{ V}$

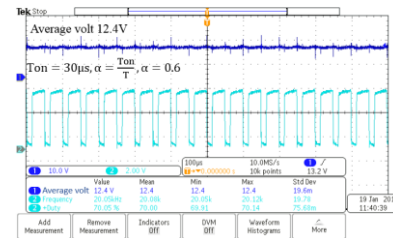
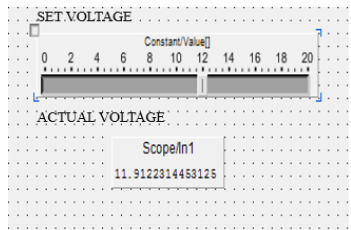


Fig 11. a. Set voltage and actual voltage in control desk

Fig. 11. b. Duty cycle and output average voltage

Fig. 11 Experimental results for  $V_o = 12$  V

## 6 SPWM Generation

The SPWM pulses for power electronic DC-AC converter are generated using simple simulink blocks in RTI library as shown in Fig 12. For SPWM generation, sinusoidal signal is used as a reference signal and remaining procedures remain same. Fig. 13 shows the SPWM pulse generation for DC-AC converter using MATLAB simulink blocks. The sinusoidal reference signal amplitude is 0.8 with a frequency of 50 Hz and phase delay is 0. Sine wave 1 and sine wave 2 are phase shifted by  $120^\circ$ . The repeating sequence is used to generate carrier switching frequency at 5 kHz. The output is directly connected with DAC which is available in master PCC in RTI library. The MATLAB pulse output is available from the corresponding output pins in DAC. A delay block is used to generate a dead time in simulink for three phase pulse generation. The switching frequency is 5 kHz and the dead time is  $10\mu\text{s}$  for the switches in the same leg which is shown in Fig. 14. The three phase input sine signal and SPWM pulses are measured by MDO\_3143.

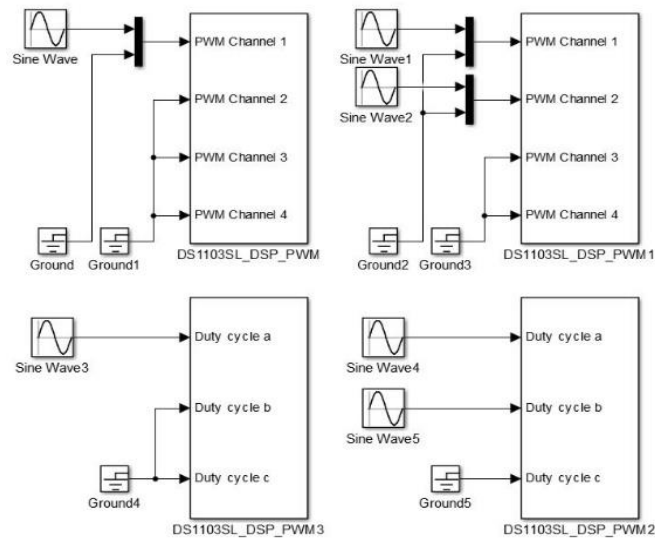


Fig 12. SPWM generation DC to AC converter

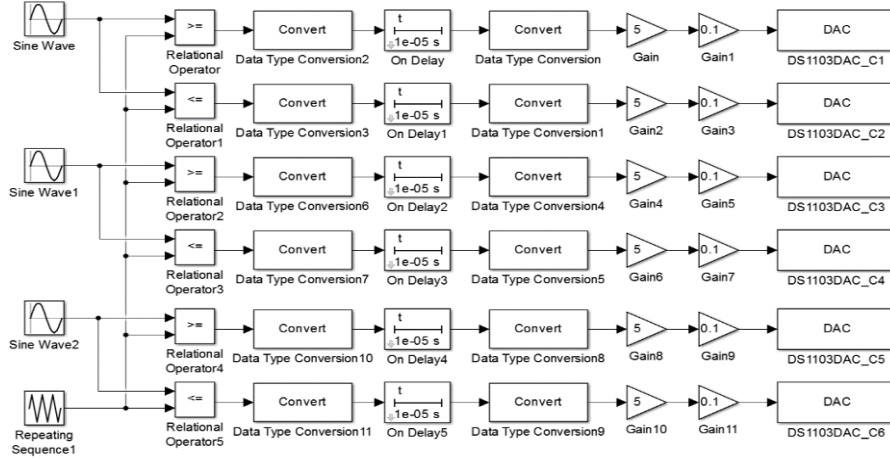


Fig 13. 3-phase SPWM generation using MATLAB Simulink

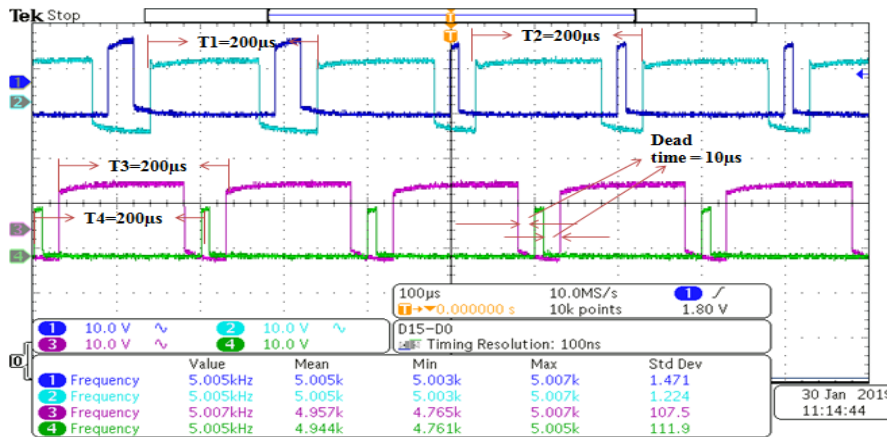


Fig 14. 3-phase SPWM waveforms with dead time

## 7 Experimental Setup for DC-AC Converter

Fig. 15 shows the overall experimental set up of a 3-phase inverter fed induction motor with brake drum arrangements controlled by dSPACE 1103 controller. NI9225 voltage sensor and NI9227 current sensor are used to measure 300 V rms and 5 A rms respectively. An uncontrolled 3-phase rectifier 50A, 1200V is used to supply AC-DC input to the 3-phase inverter. The dc link capacitor of 450 V, 220  $\mu$ F is used to minimise the dc ripples. The 3-phase SPWM signal generated from the dSPACE1103 chip is connected to the 3-phase inverter (IGBT) via DAC pins. Fig. 16 shows the 3-phase rectifier input current waveform, output load current and voltage waveform of a 3-phase induction motor load. The waveforms are observed using NI DAC LabVIEW software program

in front panel. The speed is sensed by proximity sensor and the simulink blocks necessary to measure the speed are provided in Fig. 17. The observed proximity sensor output and the corresponding speed waveform are measured in control desk as shown in Fig. 18.

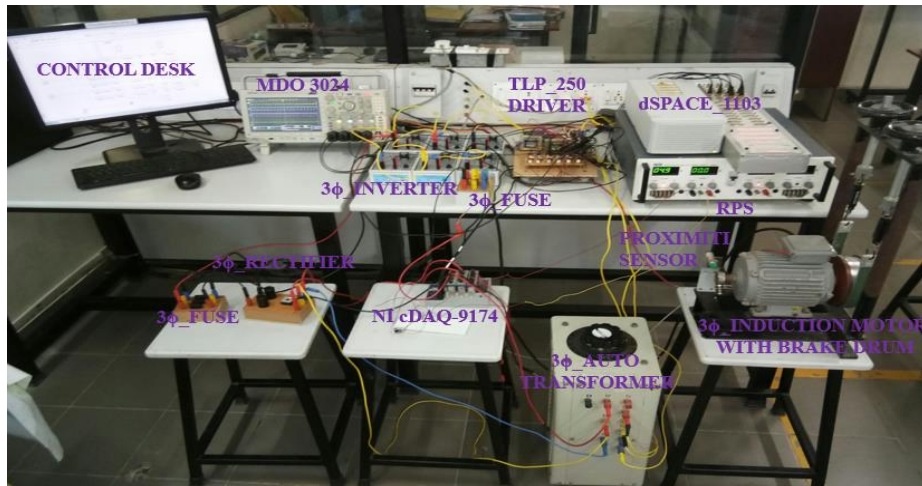


Fig 15. Experimental setup for inverter fed induction motor drive

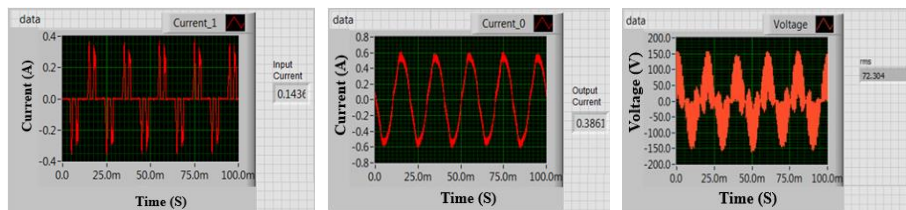


Fig 16. a. Input current

Fig 16. b. Output current

Fig 16. c. Output voltage

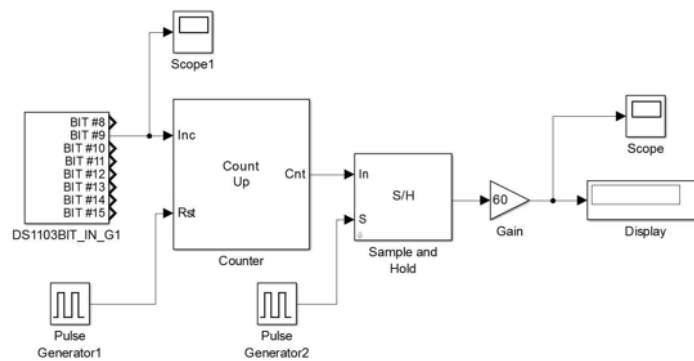


Fig 17. RPM measurement in simulation

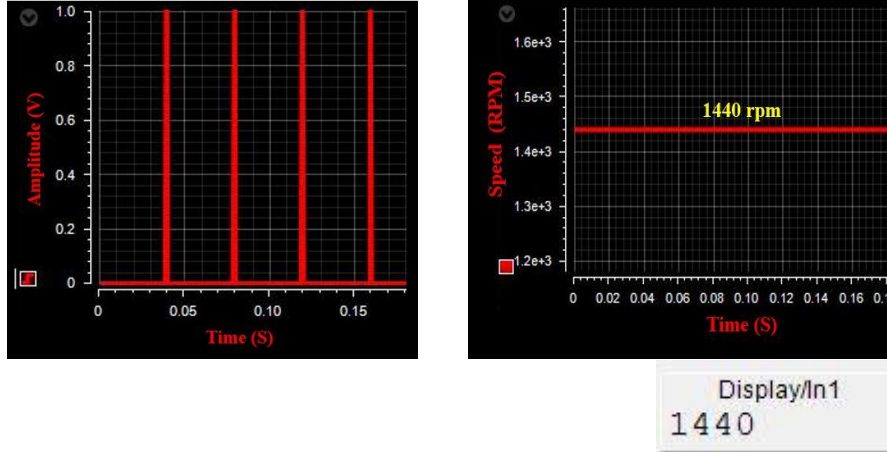


Fig 18. Proximity sensor output and speed waveform in control desk

## 8 Conclusion

The overview, working procedure, configuration and control desk parameter settings of dSPACE1103 controller are presented in simple steps for PWM generation using RTI library. It will be much helpful for young researchers and engineers to learn the working procedure in dSPACE easily. The PWM for duty cycle control of DC-DC converter is presented with experimental results. The closed loop control of DC-DC converter was demonstrated without additional hardware components for PI controller and other control circuits. The SPWM for voltage and frequency control of DC-AC converter is demonstrated with induction motor drive using RTI library blocks in dSPACE and MATLAB simulink blocks. The preference of different PWM blocks in RTI library depends upon the user requirement. The dSPACE1103 controller can be used to generate the switching pulses at high frequency (above 100 kHz).

## References

1. H. Chen, M. Yen, Q. Wu, K. Chang, L. Wang, "Batteryless transceiver prototype for medical implant in 0.18- m CMOS technology," *Microwave Theory and techniques IEEE Transaction on*, vol. 62, no. 1, pp. 137–147, Jan 2014.
2. S. Cui, I. S. N. Soltau, R. W. De Doncker, "A high step-up ratio soft-switching DC-DC converter for interconnection of MVDC and HVDC grids," *IEEE Trans. Power Electron*, vol. 33, no. 4, pp. 2986–3001, April 2018.
3. S. P. Engel M. Stieneker, N. Soltau, S. Rabiee, H. Stagge, R. W. De Doncker, "Comparison of the modular multilevel DC converter and the dual-active Bridge converter for power conversion in HVDC and MVDC grids," *IEEE Trans. Power Electron*, vol. 30, no. 1, pp. 124–137, Jan 2015.

4. Ebrahim B, Okhtay A, "A new topology for bidirectional multi-input multi-output buck direct current–direct current converter", *Int. Trans. Electr. Energ. Syst.*, vol. 27, no. 2, pp. e2254, Feb. 2017.
5. A. A. Samson, A. S. Kumar, "Design and Analysis of Fuel Cell for Standalone Renewable Energy System," *IEEE national conference on emerging trends in new & renewable energy sources and energy management (NECT NRES EM)*, pp. 170–175, Dec 2014.
6. A. Tani, M. B. Camara, B. Dakyo, Y. Azzouz, "DC/DC and DC/AC converters control for hybrid electric vehicles energy and fuel cell," *IEEE Trans. Ind. Inform.* vol. 9, no. 2, pp. 686–696, May 2013.
7. Y. Lee, A. Khaligh, A. Emadi, "Advanced integrated bidirectional AC/DC and DC/DC converter for plug-in hybrid electric vehicles," *IEEE Trans. Veh. Technol.*, vol. 58, no. 8, pp. 3970–3980, Oct 2009.
8. V. V. Subrahmanya Kumar Bhajana, P Drabek and Pramod Kumar A, "Design and implementation of a zero voltage transition bidirectional DC-DC converter for DC traction vehicles", *Int. Trans. Electr. Energ. Syst.*, <https://doi.org/10.1002/2050-7038.2842>.
9. H. Lee, J. Yun, "High-efficiency bidirectional buck-boost converter for photovoltaic and energy storage systems in a smart grid," *IEEE Trans. Power Electron.*, vol. 34, no. 5, pp. 4316-4328, May 2019.
10. B. M. Han, N. S. Choi, J.Y. Lee, "New bidirectional intelligent semiconductor transformer for smart grid application," *IEEE Trans. Power Electron*, vol. 29, no. 8, pp. 4058–4066, Aug 2014.
11. B. Sri Revathi, M. Prabhakar, F. G. Longatt, "High-gain–high-power (HGHP) DC-DC converter for DC microgrid applications: Design and testing" *Int. Trans. Electr. Energ. Syst.*, vol. 8, no.2, pp. e2483, Feb. 2018.
12. Q. Chen, N. Liu, C. Hu, "Autonomous energy management strategy for solid state transformer to integrate PV-assisted EV charging station participating in ancillary service," *IEEE Trans. Ind. Inform.* vol. 13, no. 1, pp. 258-269, Feb 2017.
13. X. Yu, X. She, X. Zhou, "Power management for DC microgrid enabled by solid-state transformer," *IEEE Trans. Smart Grid.*, vol. 5, no. 2, pp. 954–965, March 2014.
14. H. M. de Oliveira Filho, D. de Souza Oliveira, P. P. Praça, "Steady- state analysis of a ZVS bidirectional isolated three-phase DC-DC converter using dual phase-shift control with variable duty cycle," *IEEE Trans. Power Electron*, vol. 31, no. 3, pp. 1863-1872, March 2016.
15. S. Mehrnami, S. K. Mazumder, H. Soni, "Modulation scheme for three-phase differential-mode Čuk inverter," *IEEE Trans. Power Electron*, vol. 31, no. 3, pp. 2654-2668, March 2016.
16. Z. Liang, X. Lin, Y. Kang, B. Gao, H. Lei, "Short circuit current characteristics analysis and improved current limiting strategy for three-phase three-leg inverter under asymmetric short circuit fault," *IEEE Trans. Power Electron.*, vol. 33, no. 8, pp. 7214-7228, Aug 2018.
17. B. Tamyurek, "A high-performance SPWM controller for three-phase UPS systems operating under highly nonlinear loads," *IEEE Trans. Power Electron.*, vol. 28, no. 8, pp. 3689-3701, Aug 2013
18. Y. Song, B. Wang, "A survey on reliability of power electronic systems," *IEEE Trans. Power Electron.*, vol. 28, no. 1, pp. 7214-7228, Jan 2013.
19. K. A. Chinmaya and Girish Kumar Singh, "Experimental analysis of various space vector pulse width modulation (SVPWM) techniques for dual three-phase induction motor drive", *Int. Trans. Electr. Energ. Syst.*, <https://doi.org/10.1002/etep.2678>.
20. P. Sun, C. Liu, J. Lai, "Three-phase dual-buck inverter with Unified Pulse width Modulation," *IEEE Trans. Power Electron.*, vol. 27, no. 3, pp. 7214-7228, Mar 2012.

21. Z. Housheng, Z. Yanlei, "Research on a novel digital photovoltaic array simulator," International Conference on Intelligent Computing Technology and Automation. pp. 1077–1080, May 2010.
22. D. D. C. Lu, Q. N. Nguyen, "A photovoltaic panel emulator using a buck-boost DC/DC converter and a low cost micro-controller," Sol. Energy, vol. 86, no. 5, pp. 1477–1484, 2012.
23. P. Fajri, S. Lee, P. V. Anand Kishore, M. Ferdowsi, "Modeling and integration of electric vehicle regenerative and friction braking for motor/dynamometer test bench emulation," IEEE Trans. Veh. Technol., vol. 65, no. 6, pp. 4264–4273, 2016.
24. Subrata B, Arnab G, Sanjeevikumar P, "Modeling and analysis of complex dynamics for dSPACE controlled closed-loop DC-DC boost converter" Int. Trans. Electr. Energ. Syst., <https://doi.org/10.1002/etep.2813> (available online from Jan.2019).
25. A. Gebregergis, P. Pillay, "Implementation of fuel cell emulation on DSP and dSPACE controllers in the design of power electronic converters," IEEE Trans. Ind. Appl., vol. 46, no. 1, pp. 285-294, Jul./Feb. 2010.
26. M. R. Sarker, R. Mohamed, "dSPACE controller-based enhanced piezoelectric energy harvesting system using PI-lightning search algorithm," IEEE Access, vol. 7, pp. 3610–3626, 2019.
27. S. M.Azharuddin, M.Vysakh, H. V.Thakur, B. Nishant, T. Sudhakar Babu, K.Muralidhar, Don Paul, B. Jacob, K. Balasubramanian, N. Rajasekar, "A near accurate solar PV emulator using dSPACE controller for real-time control," Energy Procedia, vol. 61, pp. 2640–2648, 2014.
28. R. V Meshram, M. Bhagwat, S. Khade, S. R. Wagh, A. M. Stankovi, N. M. Singh, "Port-controlled phasor hamiltonian modeling and IDA-PBC control of solid-state transformer," IEEE Trans. Control Syst. Technol., vol. 27, no. 1, pp. 349–356, Jan. 2019.
29. T. Hac, S. Karaman, E. Kural, E. S. Öztürk, M. Demirci, B. A. Güvenç, "Adaptive headlight system design using hardware-in-the-loop simulation," IEEE International Conference on Control Applications., pp. 915–920, 2006.
30. A. Thomas, A. W. Anakwa, "dSPACE DS1103 control workstation tutorial and DC motor speed Control Tutorial," 2009.uthor, F.: Article title. Journal 2(5), 99–110 (2016).